THE JOURNAL OF PHYSICAL CHEMISTRY B

Article

Cite This: J. Phys. Chem. B 2019, 123, 7103−7112

pubs.acs.org/JPCB

Measuring Intrinsic Disorder and Tracking Conformational Transitions Using Rosetta ResidueDisorder

Justin T. Seffernick,[†] He Ren,[‡] Stephanie S. Kim,[†] and Steffen Lindert*[,†]

[†]Department of Chemistry and Biochemistry, Ohio State University, Columbus, Ohio 43210, United States

[‡]Department of Chemistry/Biochemistry, Oberlin College, Oberlin, Ohio 44074, United States

Supporting Information

ABSTRACT: Many proteins contain regions of intrinsic disorder, not folding into unique, stable conformations. Numerous experimental methods have been developed to measure the disorder of all or select residues. In the absence of experimental data, computational methods are often utilized to identify these disordered regions and thus gain a better understanding of both structure and function. Many freely available computational methods have been developed to predict regions of intrinsic disorder from the primary sequence of a protein, including our recently developed Rosetta ResidueDisorder. While these methods are very useful, they are only designed to predict intrinsic disorder from the sequence. However, it would be useful to have a method that could also measure intrinsic disorder directly from structure. Such a method might also be used to identify changes in the structure of systems that can transition from folded to unfolded or vice versa, even systems that are not intrinsically disordered. Here we extended the capabilities of Rosetta ResidueDisorder to measure the intrinsic disorder from the coordinates of a single conformation of a protein. As a proof of principle, we show that ResidueDisorder can measure the intrinsic disorder from the coordinates with a higher accuracy (69.2%) than when predicted from sequence (65.4%) using a benchmark set of 229 proteins, showing that intrinsic disorder can be measured accurately from single structures over a large range of intrinsic disorder (0−100%). Additionally, we used ResidueDisorder to analyze unfolding trajectories of 12 fast-folding, nonintrinsically disordered proteins generated using molecular dynamics (MD), specifically steered MD (SMD), high-temperature MD, and accelerated MD (aMD) as well as long-time scale folding/unfolding trajectories. Using ResidueDisorder, a clear correlation between RMSD with respect to the native structure and measured fraction of denatured residues was observed. Finally, we introduced methods to predict folding/unfolding transitions as well as a native-like structure in the absence of a crystal structure from folding/unfolding MD trajectories. Rosetta ResidueDisorder is available as an application in the Rosetta software suite with the addition of new capabilities for directly identifying denatured regions and predicting events.

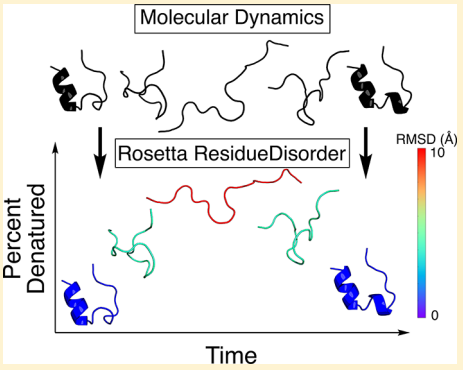

INTRODUCTION

Over the last number of years, intrinsically disordered proteins (IDP) and intrinsically disordered regions (IDR) within proteins have become very active fields of study.[1−6] Although proteins are often thought to fold into stable structures encoded by the primary amino acid sequence, as evidenced by the hundreds of thousands of crystal structures in the protein databank, in reality, proteins commonly contain segments of intrinsic disorder. Disordered segments have relatively flat free energy surfaces, which causes enhanced flexibility and an ensemble of tertiary structures to be present at equilibrium.[7] These regions are frequently significant to the function of IDPs and are thus important to characterize but difficult to model computationally. Nonetheless, some progress has been made in modeling one of the most regularly studied IDPs, α-synuclein (involved in Parkinson's disease), using Monte Carlo simulations in PyRosetta.[6] Because of the importance of IDRs to biological function, many methods have been developed to predict the intrinsically disordered regions of proteins based on the primary sequence. Some commonly used methods include IUPred,[8] PrDOS,[9] DISOPRED,[10] PONDR,[11] Meta-Disorder,[12] and MFDp2.[13] Although the algorithms differ, most take advantage of the fact that disordered regions often contain a higher percentage of charged and hydrophilic residues and have low sequence complexity. In general, most of the available methods use some combination of machine learning, energy function, local secondary structure prediction, and/or homologous sequences. Recently, we developed Rosetta ResidueDisorder,[14] which uses Rosetta to predict an ensemble of tertiary structures from the primary sequence and predicts intrinsic disorder of each residue based on average scores over those conformations. Using an independent benchmark set of 229 proteins, Rosetta ResidueDisorder outperformed all six other tested methods in terms of prediction accuracy. While all of these prediction methods can be very powerful, they are only designed to predict

Received: May 7, 2019
Revised: July 12, 2019
Published: August 14, 2019

DOI: 10.1021/acs.jpcb.9b04333
J. Phys. Chem. B 2019, 123, 7103−7112

intrinsic disorder from the primary sequence. With the exception of our new developments of ResidueDisorder, available computational tools cannot measure intrinsic disorder of a protein directly from structure.

Experimentally, disorder can be measured using a variety of techniques that can be useful depending on the situation.[1] Some methods measure the intrinsic disorder of proteins by identifying residues in IDRs, which would be present in many different conformations in equilibrium. The technique that was first developed to probe intrinsic disorder was measuring sensitivity to proteolysis, where enzymes such as subtilisin, thermolysin, chymotrypsin, and trypsin tend to selectively cleave regions with a higher probability in disordered regions than in ordered regions. Using known IDPs and structured proteins as controls, disorder can be measured based on the ability of proteases to cleave peptide bonds.[15] Another commonly used technique to measure intrinsic disorder is solution nuclear magnetic resonance (NMR), which can be used to obtain an ensemble of tertiary structures that are then used to probe disorder. Often residues with RMSF (root-mean-square fluctuation) > 2 Å are defined as disordered.[16] Additionally, X-ray crystallography can sometimes be used to infer intrinsically disordered regions, which frequently present as unresolved segments in crystal structures. Other methods can measure changes in disorder of dynamic systems resulting from some event (often a binding or aggregation event). Electron paramagnetic resonance (EPR) can probe the disorder of a specific residue over an event by measuring the mobility (and thus disorder) of a cysteine (or any amino acid mutated to a cysteine) when a spin-labeled moiety is attached.[17] For example, EPR was used to measure the transition from disordered to ordered of the C-terminal region of measles nucleoprotein when it binds to the measles virus phosphoprotein.[18] Finally, Raman spectroscopy has also been used to measure disorder during the aggregation of intrinsically disordered α-synuclein into ordered fibrils, which occurs in Parkinson's disease.[19] This method takes advantage of differences in vibrational frequencies between the disordered soluble α-synuclein and the ordered fibril α-synuclein. While these methods can quantify disorder of a protein experimentally, to our knowledge, there is no computational technique that can directly quantify intrinsic disorder as a function of the coordinates of a protein. We hypothesized that such a method could then be used to identify changes in structure and to examine events from molecular dynamics (MD) trajectories, such as folding/unfolding or potentially binding events even for proteins that are not intrinsically disordered.

Rosetta, a software suite originally developed for protein structure prediction, contains algorithms for various methods to study biomolecules such as protein folding, homology modeling, loop modeling, docking, protein design, etc.[20−31] At the heart of most of Rosetta's algorithms is its all-atom energy function,[22] which approximates the energy of a three-dimensional protein structure using Rosetta Energy Units (REU), which roughly correspond to kcal/mol. This energy function was used in our developed intrinsic disorder predictor Rosetta ResidueDisorder.[14] We hypothesized that low, i.e., more energetically favorable, Rosetta scores would correspond to ordered regions and high, i.e., less energetically favorable, Rosetta scores would correspond to disordered regions. Beginning from the primary sequence, 100 de novo structures were generated using the Rosetta ab initio structure prediction. Next, each residue was scored using the Rosetta energy function (talaris2014 weights) and averaged over the 100 predicted structures. An order score was then calculated by averaging the raw Rosetta score over a window of 5 residues in both directions in order to smooth out the energy surface. Finally, residues were predicted as ordered if the order score was <−1.0 Rosetta Energy Units (REU) and disordered if the order score was >−1.0 REU. If the protein was predicted to be less than 60% disordered, a terminal residue optimization was performed where the order/disorder cutoff was increased for a percentage of the terminal residues. ResidueDisorder outperformed all other tested IDP prediction methods based on our independent benchmark set presumably because of the ability to quantify long-range interactions that other purely sequence-based methods cannot. We hypothesized that we could use a similar methodology to measure the disorder of a known structure by skipping the structure prediction step in the ResidueDisorder methodology.

In this work, we successfully verified the application of ResidueDisorder to measure intrinsic disorder directly from 3D protein coordinates. Next, we used ResidueDisorder to examine protein unfolding trajectories of nonintrinsically disordered proteins using steered, high-temperature, and accelerated MD by measuring changes in denatured regions. Finally, we used ResidueDisorder to analyze long (104−486 μs) folding/unfolding trajectories for fast-folding proteins and developed methods to predict folding/unfolding events as well as a native-like structure from the trajectory.

MATERIALS AND METHODS

Validation of ResidueDisorder To Measure Protein Disorder. As a proof of principle, we first tested our hypothesis that ResidueDisorder could accurately measure intrinsic disorder from protein structures, evaluating a benchmark set of 229 proteins from a previous study.[14] This set contained proteins extracted from the protein databank with the following criteria: fewer than 150 residues, single chained, and structures determined by NMR. From the NMR ensembles, root-mean-square fluctuation (RMSF) values were calculated for each residue after alignment. The experimental disorder was defined for each residue as disordered if RMSF > 2 Å and ordered if RMSF < 2 Å as is common in the literature.[16] The test set contained 10 899 disordered and 10 674 ordered residues (within 1% of each other to avoid biasing). To measure the disorder, we first relaxed the reported representative structure for each protein using Rosetta. If a representative model was not reported, the first model was used. Those relaxed structures were input into the Rosetta ResidueDisorder application in lieu of performing ab initio structure predictions. The percent accuracy was defined as the number of residues predicted correctly divided by the total number of residues.

Protein Data Set. For the molecular dynamics (MD) trajectory analyses we used the data set of fast-folding proteins from Lindorff-Larsen et al. (see Table S1 for full description).[32] These proteins ranged from 10 to 80 residues, contained no prosthetic groups or disulfide bonds, and contained representatives from all three major structural classes (α-helical, β sheet, and mixed α/β). Of these proteins, 8/12 had either crystal or NMR structures in the protein databank, while the other four had close homologues. For the unfolding trajectories, the homologous portions of the sequences were used and for the long folding/unfolding

DOI: 10.1021/acs.jpcb.9b04333
J. Phys. Chem. B 2019, 123, 7103−7112

trajectories; the homologues from the pdb were used as the native (for RMSD calculation). These proteins did not necessarily contain intrinsically disordered regions. For example, of the five pdb structures that were NMR ensembles, each contained less than 12% of intrinsic disorder with two containing no intrinsic disorder. However, the scope of this method is not limited to IDPs only but rather any protein that can undergo a significant conformational change.

In the developed methods where this protein data set was used, ResidueDisorder was used to assign residues in each conformation as ordered or disordered using the previously described parameters.[14] Since these residues were not necessarily intrinsically disordered and can change structure over time in a simulation, we will refer to the percent of residues that were assigned as disordered by Rosetta ResidueDisorder as percentage of denatured residues. While the concepts of intrinsic disorder and denaturation are biologically very different, we hypothesized that they would have the same effect on the Rosetta energy function: residues with low scores would be more ordered or less denatured and vice versa. Thus, we hypothesized that our method Rosetta ResidueDisorder could be used to not only measure intrinsic disorder (using a single native structure or ensemble of native structures) but also track conformational changes of proteins by assigning residues as denatured or not denatured as a function of time and structure. For example, the percentage of denatured residues would decrease during a folding event. This metric was used in the evaluation of MD trajectories for proteins in this data set.

Unfolding Proteins Using MD (SMD, High-Temperature, aMD). Steered molecular dynamics (SMD)[33] was used to unfold the 12 fast-folding proteins. Each protein was solvated using visual molecular dynamics (VMD)[34] in a 14 Å padded TIP3P water box and ionized with Na^+ and Cl^-. SMD simulations were performed using the CHARMM27 force field[35] and NAMD 2.12.[36] For each protein, two minimization phases were performed: ion/water minimization for 20 000 steps followed by protein/ion/water minimization for 20 000 steps. Two equilibration steps were also performed: heating of the system to 300 K by weakening restraints followed by 20 ps equilibration. Following the minimization/equilibration, SMD was performed for 10−25 ns at constant velocity (SMD atom spring constant = 7 kcal/mol/Å, SMD velocity = 0.00002 Å/time step) where the N-terminal Cα was fixed and the C-terminal Cα was pulled in the opposite direction from the N-terminal Cα. Finally, frames every 0.2 ns were extracted from the trajectory, relaxed in Rosetta, and input into the ResidueDisorder application to determine the percentage of denatured residues.

High-temperature molecular dynamics was also used to unfold the 12 fast-folding proteins at 500 K. Proteins were solvated and minimized (as described for SMD above). However, the two equilibration phases were performed at 500 K. Following the minimization/equilibration, 200 ns MD production runs were performed at the elevated temperature (500 K). Similarly, frames every 0.2 ns were extracted from the trajectory, relaxed in Rosetta, and input into the ResidueDisorder application for determination of denatured residues.

Finally, accelerated molecular dynamics (aMD)[37,38] was furthermore used to unfold the 12 fast-folding proteins. The procedure was previously described in detail,[39] but in short, proteins were solvated, minimized, and equilibrated (as described for SMD above). Following the equilibration, a 100 ns conventional MD simulation was performed at 300 K in order to fully equilibrate the system and extract appropriate acceleration parameters. From the 100 ns conventional MD simulation, aMD parameters (E and α for both total and dihedral potentials) were extracted for each protein as previously described.[39] However, to facilitate faster unfolding, a higher boost potential was used for both total and dihedral potentials, cutting the α parameters in half. Using the calculated aMD parameters, 200 ns aMD simulations were run for each protein. Similarly, frames every 0.2 ns were extracted from the trajectory, relaxed in Rosetta, and input into the ResidueDisorder application for determination of denatured residues.

Measuring Disorder of Folding/Unfolding Events (Fast Folding Trajectories). MD trajectories of 12 fast-folding proteins were obtained from D. E. Shaw Research.[32] The simulations were performed near the respective melting temperatures of each protein and ranged from 104 to 486 μs in length. Some simulations were initiated in the folded state, while some were initiated in an unfolded state. In all simulations, multiple spontaneous folds/unfolds were observed throughout the trajectories. From these trajectories, protein coordinates were extracted every 20 ns. These frames were relaxed in Rosetta in order to equilibrate within the Rosetta energy function. Subsequently, each relaxed frame was separately input into the ResidueDisorder application, and the percentage of denatured residues was determined.

Prediction of Folding/Unfolding Events. For each extracted time point (every 20 ns) from the folding/unfolding MD trajectories, the difference in the average percentage of denatured residues for 25 steps (500 ns) before that time point and 25 steps after that time point was calculated. A cutoff line for the absolute value of the difference was instituted, above which an event was defined, representing a significant change in structure at that time point. This cutoff line was defined as 60% of the largest difference for each protein. If the percentage of denatured residues increased during the event, it was defined as an unfolding event, and if the percent of denatured residues decreased during an event, it was defined as a folding event. If events were detected in adjacent time steps, they were combined to form a single event in the center of the range.

To test the effectiveness of this prediction, we used TimeScapes,[40] a software specifically designed to detect events from MD trajectories (containing frames every 20 ns) as a comparison. To run on the trajectories, the terrain algorithm from TimeScapes was used, which performed event detection and activity monitoring. We utilized the recommended parameters: cut1, 6.0 Å; cut2, 7.0 Å; delta, 5% of total frames; gtype, Cutoff.

Prediction of Native-Like Structures from MD Simulations. To select a native-like structure from a folding/unfolding MD trajectory, the percentage of denatured residues was first smoothed for each frame by calculating the average using a window of 50 time steps (1 μs) in both directions. On the basis of this analysis, we selected frames in highly structured regions (i.e., low window-averaged percent denatured). We hypothesized that the lower the fraction of denatured residues for a structure, the more native-like the structure would be, even for proteins that do contain some intrinsically unstructured regions (i.e., intrinsic disorder). Next, the 5% of structures containing the fewest denatured residues based on the window average were extracted. The extracted structures were then clustered using MaxCluster[41] with the

DOI: 10.1021/acs.jpcb.9b04333
J. Phys. Chem. B 2019, 123, 7103−7112

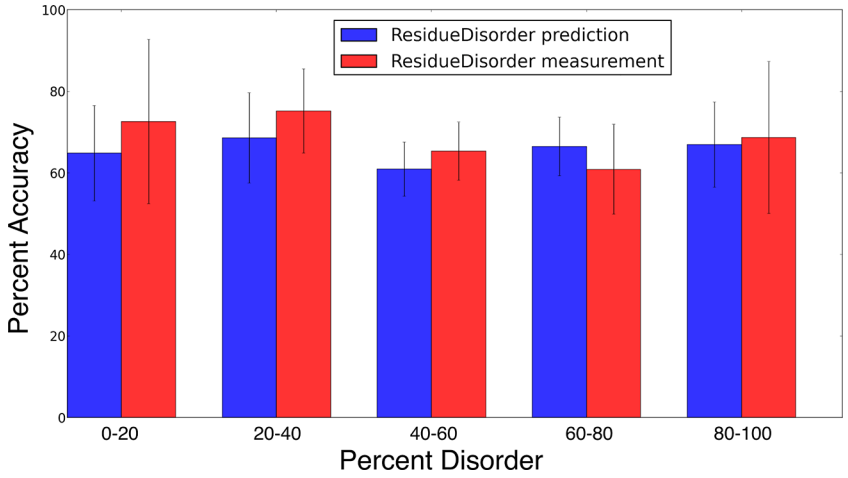

Figure 1. Percent accuracy of Rosetta ResidueDisorder on a benchmark set of 229 NMR proteins when used to predict intrinsic disorder from sequences and measure intrinsic disorder using reported representative models. ResidueDisorder was consistently accurate over all levels of disorder and was more accurate when used to measure than predict in 4/5 categories. Overall, ResidueDisorder was more accurate when measuring disorder (69.2%) than predicting (65.4%)

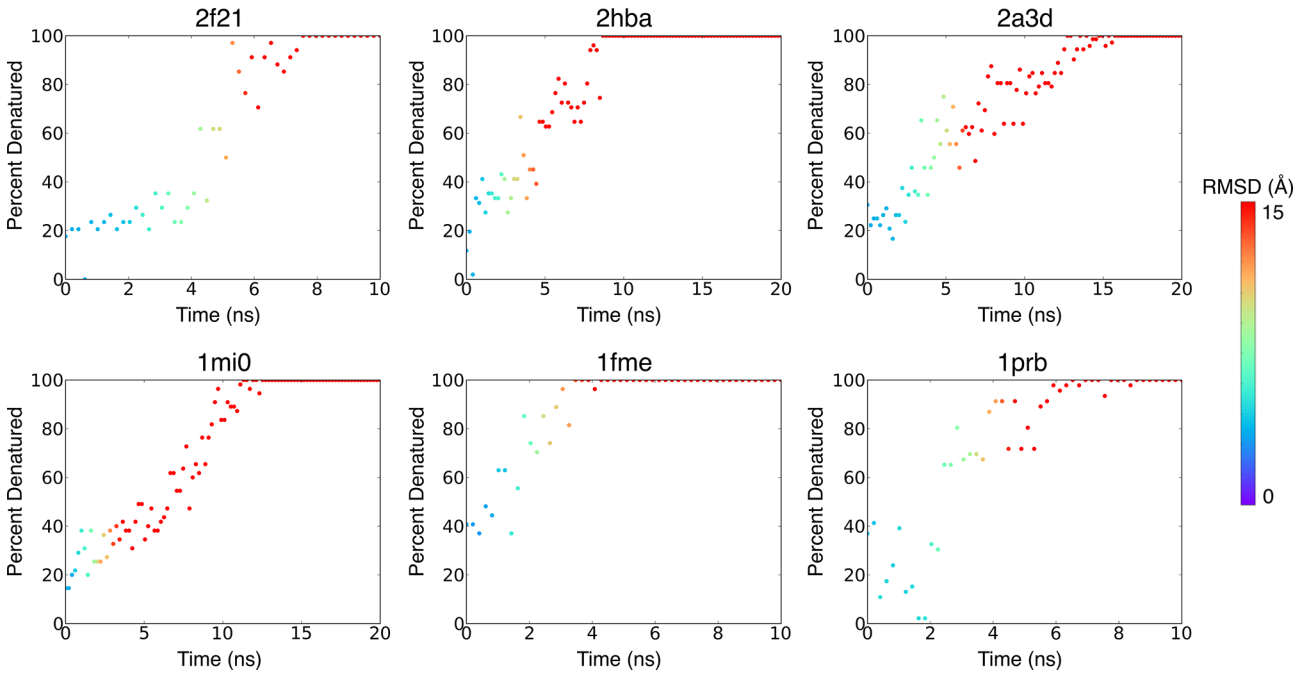

Figure 2. SMD (10−25 ns simulations) percent denatured vs time plots for the unfolding of six proteins (2f21, 2hba, 2a3d, 1mi0, 1fme, and 1prb). Color of the data points represents RMSD to the native structure (or closest homologue) for each frame. Figure S1 shows data for the remaining six proteins. As each protein unfolded, the percentage of denatured residues increased until the protein reached 100% denatured and constituted an extended chain.

neighbor pairs cluster method and a cluster radius of 0.01 Å. The final selected structure was the lowest scoring (Rosetta, after relaxation) structure in the largest identified cluster.

RESULTS AND DISCUSSION

ResidueDisorder Measures Intrinsic Disorder More Accurately than Prediction from Sequence. Using the benchmark set from a previous study,[14] which contained 229 protein structures determined by NMR, we first tested our hypothesis that ResidueDisorder could be used to measure the intrinsic disorder from a known structure rather than predicting the disorder from an amino acid sequence. When ResidueDisorder was used on the predicted ensemble of tertiary structures (from sequence using Rosetta ab initio protein folding to generate structures), the accuracy in disorder prediction was 65.4%, which outperformed six other available disorder prediction methods in our previous study.[14] When the NMR representative models were relaxed in Rosetta and input into ResidueDisorder instead of predicted structures, the accuracy increased to 69.2%. ResidueDisorder made consistently accurate predictions over all levels of disorder. Figure 1 shows the percent accuracy for all levels of disorder (0−20%, 20−40%, 40−60%, 60−80%, and 80−100%) when ResidueDisorder was used to predict and measure disorder. In addition to being consistent over all levels of disorder (within 15%), the accuracy for measuring was higher than for predicting for four

DOI: 10.1021/acs.jpcb.9b04333
J. Phys. Chem. B 2019, 123, 7103−7112

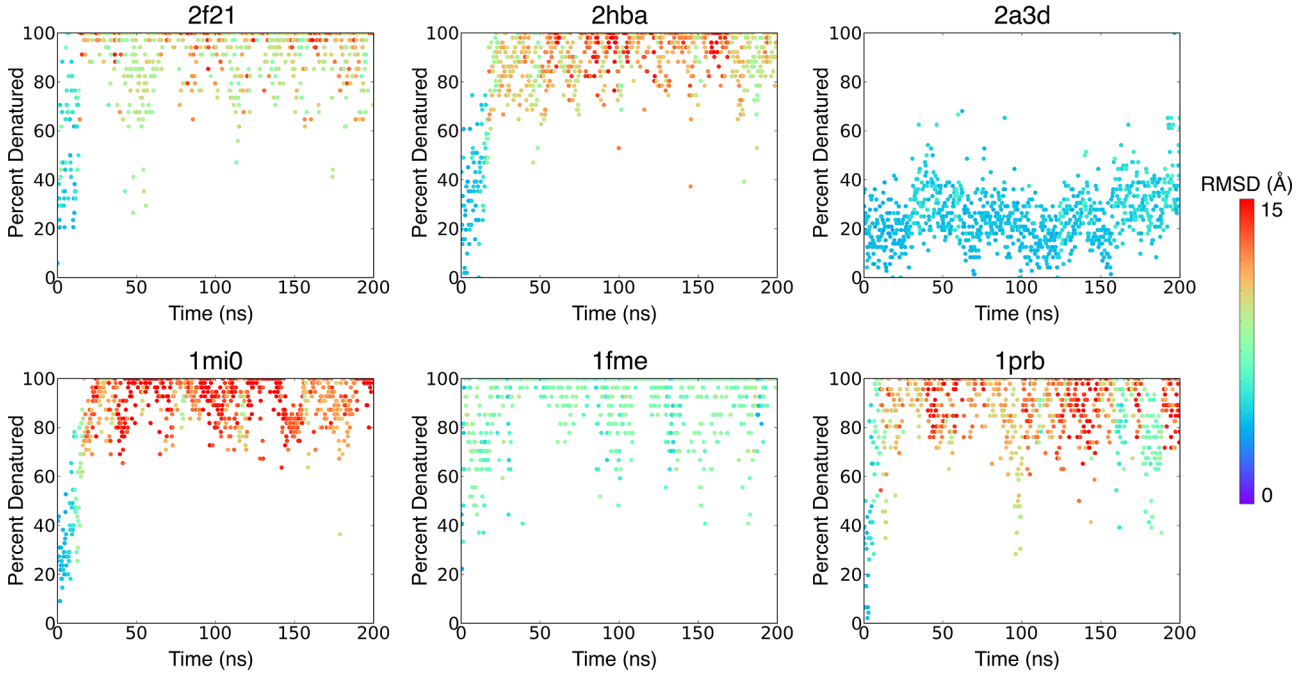

Figure 3. High-temperature (500 K) MD (200 ns simulations) percent denatured vs time plots for the unfolding of six proteins (2f21, 2hba, 2a3d, 1mi0, 1fme, and 1prb). Color of the data points represents RMSD to the native structure (or closest homologue) for each frame. Figure S2 shows data for the remaining six proteins.

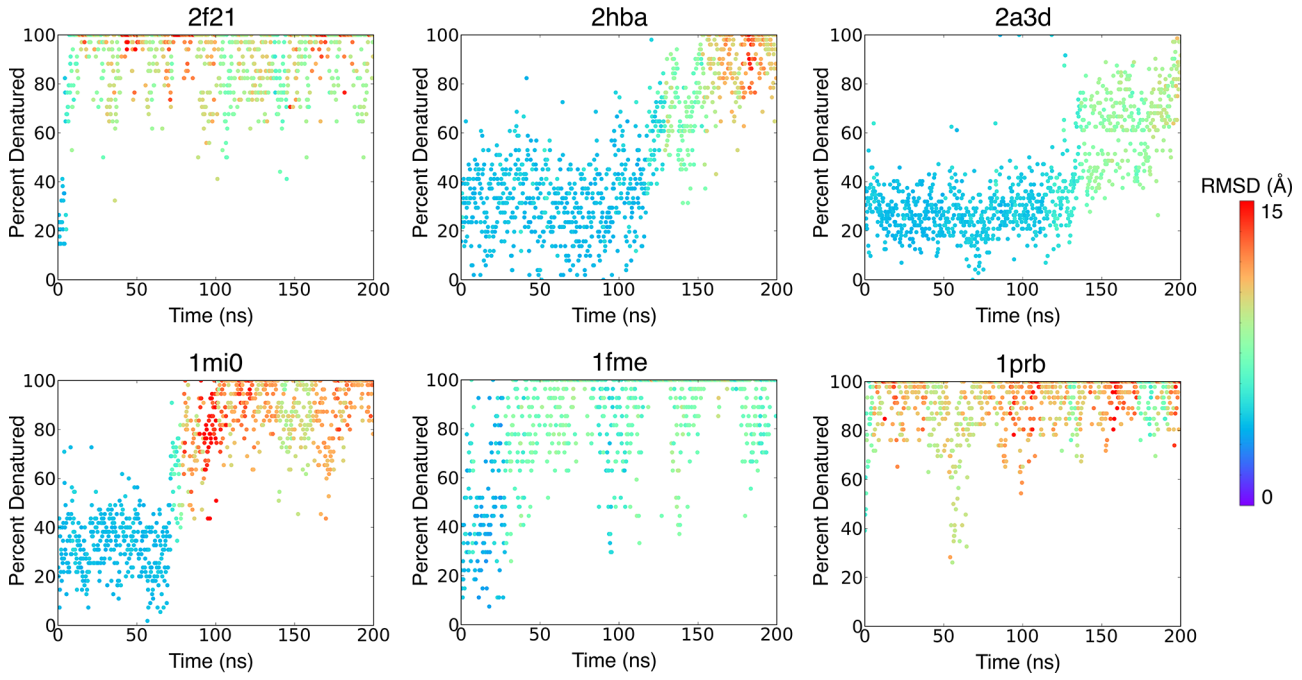

Figure 4. Accelerated MD (200 ns simulations) percent denatured vs time plots for the unfolding of six proteins (2f21, 2hba, 2a3d, 1mi0, 1fme, and 1prb). Color of the data points represents RMSD to the native structure (or closest homologue) for each frame. Figure S3 shows data for the remaining six proteins.

out of five levels of disorder. When all NMR models were input into ResidueDisorder (averaging raw Rosetta scores over all the models before calculating order scores), the accuracy only further increased to 69.8%. Interestingly, including the additional models only slightly improved the accuracy. This suggests that ResidueDisorder can accurately measure disorder using a single structure as input, not needing an ensemble of structures. In addition to the NMR data set, ResidueDisorder was also able to accurately measure intrinsic disorder from the structure for the 16 protein training set.[14] The accuracy improved from 71.8% when predicted to 74.6% when measured. These results were note surprising as using the actual structures to measure the disorder reduced the noise from predicting the structures. This analysis served as a proof of principle for our next hypothesis, that the same method

DOI: 10.1021/acs.jpcb.9b04333
J. Phys. Chem. B 2019, 123, 7103−7112

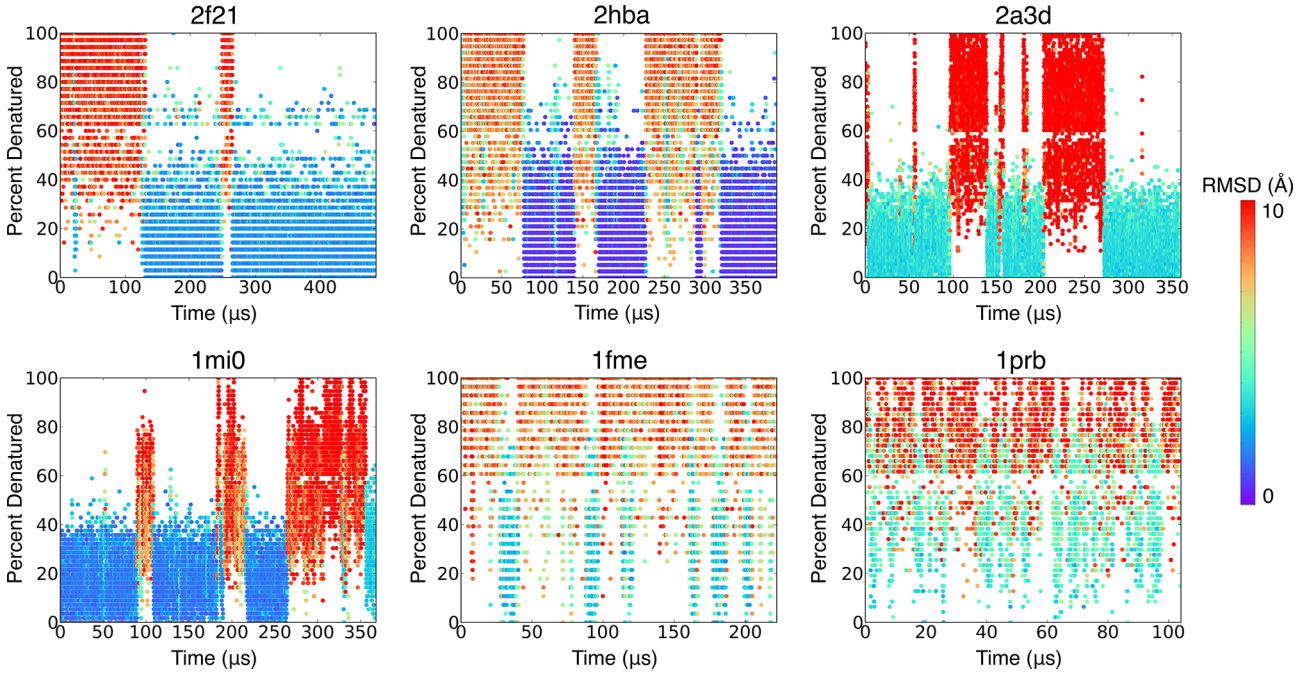

Figure 5. Percent denatured vs time plots for the trajectories of six fast folding proteins (2f21, 2hba, 2a3d, 1mi0, 1fme, and 1prb). Figure S4 shows data for the remaining six proteins. Color of the data points represents RMSD to the native structure (or closest homologue) for each frame. Rosetta ResidueDisorder separated the folded (low RMSD) states from the unfolded (high RMSD) states based on percentage of denatured residues. Highly nondenatured regions corresponded to low RMSD (folded) and highly denatured regions corresponded to high RMSD (unfolded).

could be applied to individual structures to track changes throughout a conformational change.

Unfolding Proteins Using MD (SMD, High-Temperature MD, and AMD) and Tracking Conformational Transitions. Steered molecular dynamics (SMD) was performed for each of the 12 fast-folding proteins (2rvd, 2jof, 1fme, 2f4k, 2f21, 2hba, 2wxc, 1prb, 2p6j, 1mi0, 2a3d, and 1lmb) that did not necessarily contain intrinsically disordered regions. Each simulation started in the nondenatured, folded state (as they were obtained from pdb structures). For each simulation, the C-terminal end was pulled away from the N-terminal end with a constant velocity, which unfolded the proteins. Frames were extracted every 0.2 ns, and the percentage of denatured residues was measured using ResidueDisorder as a function of the simulation time. All simulations showed that as the protein unfolded over time, the amount of denaturation also increased, as shown in Figures 2 and S1. This was due to the loss of favorable interactions and secondary structure which are rewarded by the Rosetta energy function, resulting in ResidueDisorder assigning more residues as denatured. At some point in each simulation the protein unfolded to form an extended chain, which constituted a completely denatured state. Figures 2 and S1 also show RMSD values to the native structure at each time point as a heatmap. Percentage of denatured residues correlated well with RMSD for these simulations.

In order to probe a more realistic denaturation pathway, high-temperature MD simulations were also performed for the 12 fast-folding proteins at 500 K for 200 ns. Figures 3 and S2 show the measured percent denatured vs time plots over the simulations as well as the RMSD for each frame. The proteins generally unfolded during the 200 ns. Similarly to the SMD trajectories, the amount of denatured residues correlated well with the RMSDs. While most proteins did unfold quickly within the 200 ns, 2a3d remained mostly folded (relatively small changes in RMSD). However, the percent denatured also stayed relatively constant throughout the simulation.

Finally, accelerated molecular dynamics simulations (aMD) were also performed using a high boost potential. Figures 4 and S3 show the percent denatured vs time plots for the aMD trajectories. Because of the high boost potential allowing for the sampling of high-energy conformations faster, unfolding was observed in all cases. Again, all of these unfolding events (evidenced by large increases in RMSD) corresponded to large increases in the denatured fraction of residues.

Tracking Conformational Changes of Folding/Unfolding Events (Fast-Folding Trajectories). Fast-folding protein MD trajectories were obtained from D. E. Shaw Research.[32] These simulations were initiated from either folded or unfolded states, were performed near the melting temperatures, and ranged from 104 to 486 μs (see Table S1 for details). Each trajectory contained multiple folding/unfolding events (transitions with decreases/increases in denaturation, respectively). From these trajectories, frames were extracted every 20 ns, relaxed in Rosetta, and input into the ResidueDisorder application to measure the instantaneous fraction of denatured residues for each frame. Percent denatured vs time plots, Figures 5 and S4, show that there was a correlation between low denaturation and low RMSD (plotted as a heatmap). In general, low RMSD regions (blue) were less denatured than high RMSD regions (red) for each trajectory. The average RMSD of frames with fewer than 5% denatured residues was 1.9 Å, while the average RMSD of all frames with more than 90% denatured residues was 9.1 Å. Average RMSDs over the whole range of denaturation are shown in Table 1. Figure S5 shows the percent denatured residues vs RMSD for all frames. There was a trend that low RMSD structures generally had a lower fraction of denatured

DOI: 10.1021/acs.jpcb.9b04333
J. Phys. Chem. B 2019, 123, 7103−7112

Table 1. Average RMSDs (Angstroms) over a Range of Structures for All Proteins from the Fast-Folding MD Trajectories[32] [a]

range of percent denatured	average RMSD (Å)
0–5	1.8
0–10	2.0
10–20	2.6
20–30	3.8
30–40	5.9
40–50	7.5
50–60	8.0
60–70	8.5
70–80	9.0
80–90	9.3
90–100	9.1

[a]Average RMSD increases as the percentage of denaturation increases.

residues, as also evidenced by the data in Table 1. As can be seen in Figure 5, not every high RMSD frame was also highly denatured, and conversely, not every low RMSD frame was highly structured, but rather the frames generally separated well into regions of high or low RMSD and thus high or low fraction of denatured residues which corresponded to the unfolded and folded states, respectively. For example, consider 2f21, which started in an unfolded state with both high RMSD and fraction of denatured residues. At around a time step of 1100 (22 μs), a short-lived folded state was observed as evidenced by the low RMSD and fraction of denatured residues, followed by a rapid unfolding. Then at around time step 6300 (126 μs), the protein began to fold, unfold, and fold again, where it stayed folded until time step 12 500 (250 μs). Finally, the protein folded again at time step 13 200 (264 μs). All of these changes in conformation can be observed based on regions of high RMSD and denaturation, corresponding to an unfolded state, and regions of low RMSD and denaturation, corresponding to a folded state. On the basis of this evidence, we wanted to take advantage of the separation between folded and unfolded states to predict folding/unfolding events that occur during the trajectories in the absence of a crystal structure.

Predicting Folding/Unfolding Events. Since the ResidueDisorder-calculated percentage of denatured residues naturally separated the trajectories into folded and unfolded regions, we sought to predict these folding and unfolding events based on the measured denaturation in the absence of a native structure. To do this, the difference between the average percentage of denatured residues of the 25 timesteps before and after each time point was calculated. If the absolute value of this difference was greater than a cutoff (60% of maximum absolute value of difference for each protein), an event was defined. This event was defined as an unfolding event if the fraction of denatured residues increased and as a folding event if the fraction of denatured residues decreased. Figures 6 and S6 show the percentage of denatured residues vs time plots for six proteins with the predicted events shown with black vertical lines (dotted, unfolding; solid, folding). Visually, this prediction worked best for trajectories that had clear separation between folded and unfolded states. To further test these predictions, we used the terrain algorithm from TimeScapes, which performs event detection and activity monitoring, on the trajectory containing the same frames (every 20 ns) as a comparison. These results are also shown in Figures 6 and S6 as blue arrows. If we again consider 2f21, ResidueDisorder identified all of the previously described events and correctly identified them as either folding or unfolding (fold at time step 1101 (22 μs), unfold at time step 1220 (24 μs), fold at time step 6299 (126 μs), unfold at time step 6406 (128 μs), fold at time step 6544 (131 μs), unfold at

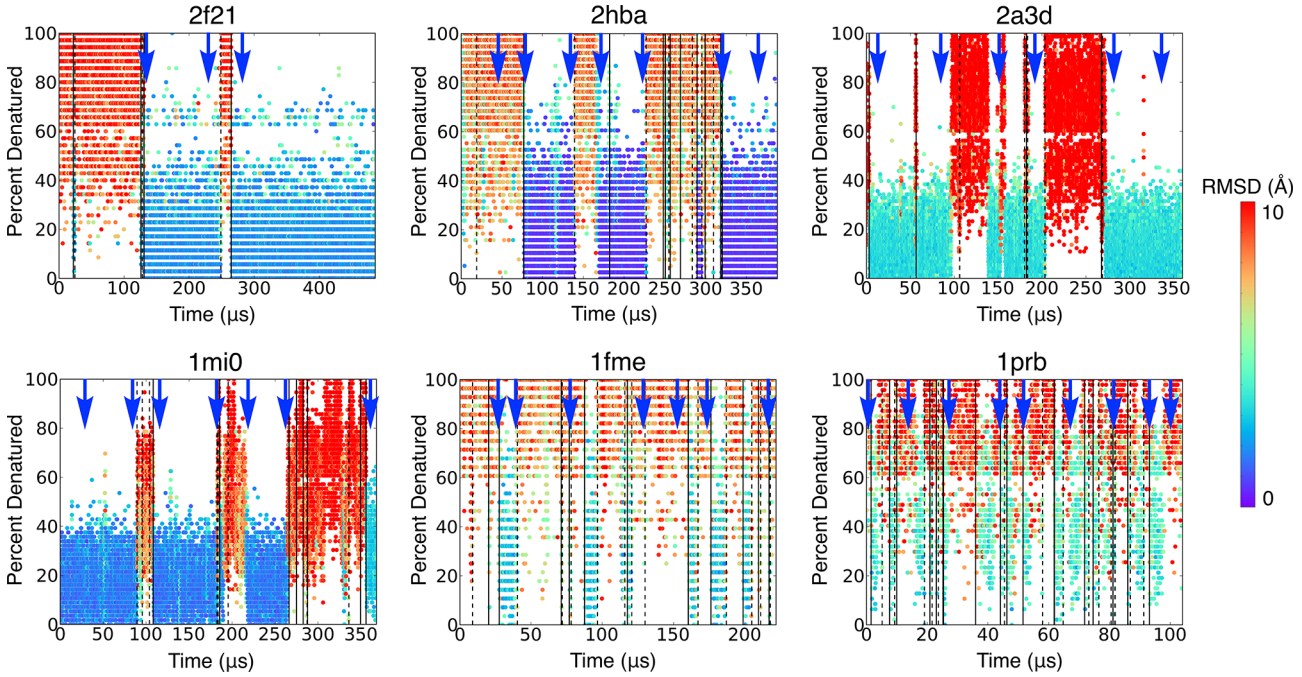

Figure 6. Percent denatured vs time plots for six fast-folding proteins (2f21, 2hba, 2a3d, 1mi0, 1fme, and 1prb) with ResidueDisorder predicted folding (solid) and unfolding (dotted) events shown as black vertical lines and TimeScapes terrain predicted events show as blue arrows for the fast folding protein trajectories. Figure S6 shows data for the remaining six proteins. RMSD to native for each frame is shown as a heatmap.

DOI: 10.1021/acs.jpcb.9b04333
J. Phys. Chem. B 2019, 123, 7103–7112

time step 12 448 (249 μs), and fold at time step 13 244 (265 μs)). TimeScapes did correctly identify the more large-scale folding/unfolding events (events at time steps 6718 (134 μs), 11 539 (231 μs), and 14 140 (283 μs)) but missed the quick fold/unfold around time step 1100 (22 μs) as well as the fold/unfold/fold transition around 6500 (130 μs), instead identifying it as a single event. Additionally, the events predicted by ResidueDisorder were much closer to the actual observed changes in RMSD for the folding around time step 12 500 (250 μs) and folding around time step 13 200 (264 μs).

For each predicted folding and unfolding event we calculated the average RMSD change for 25 steps before and after the event. The RMSD change (the difference in average RMSD for 25 steps before and 25 steps after) was −3.7 Å for predicted folding events and +3.6 Å for folding events. This indicated that our developed algorithm using ResidueDisorder successfully identified both folding and unfolding events well on average. As a comparison, the RMSD change for TimeScapes-predicted events was 1.20 Å. This event detection algorithm has been implemented in the ResidueDisorder application in Rosetta. Instructions to run this protocol can be found in the tutorial in the Supporting Information.

In addition to using ResidueDisorder to predict events based on the fraction of denatured residues, we also looked into whether we could accurately predict folding/unfolding events directly based on Rosetta score after relaxation. We performed the same calculations (as described above using ResidueDisorder), substituting Rosetta score for the percentage of denatured residues. While the accuracy of event prediction was frequently similar using these two different metrics, there were multiple cases where the usage of ResidueDisorder (which essentially discretized the Rosetta score for each residue) predicted better events than when the Rosetta score was used directly. Two examples (1fme and 2hba) are shown in Figure S7. When the Rosetta score was used to predict events (rather than the percentage of denatured residues), folding events were not detected at 27 and 160 μs for 1fme that were identified using ResidueDisorder. Additionally, for 2hba, using the Rosetta score to detect events did not detect the folding event at 77 μs or the unfolding event at 140 μs, while they were correctly detected using ResidueDisorder.

Predict Native-Like Structure from Simulation. A final application of ResidueDisorder that we explored was to select a frame from the folding/unfolding trajectory that most resembled the native crystal structure. The application of ResidueDisorder to dynamic systems does not require the system to be either intrinsically ordered or disordered. We hypothesized that although proteins can have intrinsic disorder, in general, the least denatured conformation (as measured by ResidueDisorder) sampled during the simulation should correspond to the most native-like structure even if the native structure has some intrinsic disorder. To do this, we calculated a window average (50 time steps in both directions) for each time step and selected the 5% of lowest window-averaged denatured frames. Using these frames from highly structured regions, we performed a clustering analysis in order to select the most representative structure. We selected the lowest (Rosetta) scoring frame from the largest cluster as the native-like structure. We used the RMSDs from the Lindorff-Larsen et al. clustering analysis of these trajectories as a comparison to the selection method from ResidueDisorder. Most of the structures selected from ResidueDisorder had lower RMSDs than selected by Lindorff-Larsen et al. (7/12), and the average RMSD over the 12 proteins was also lower for ResidueDisorder (1.9 vs 2.1 Å). Table 2 shows the RMSDs for each protein as a comparison. We hypothesize that the removal of frames from highly denatured regions, determined using ResidueDisorder, improved the clustering by also removing high RMSD structures, thus enriching the largest cluster in low RMSD structures.

Table 2. RMSDs (Å) of Selected Structure of 12 Fast-Folding Protein MD Trajectories Comparing Cluster Analysis Performed by Lindorff-Larsen et al. and Clustering Analysis Performed by Removing Highly Denatured Frames Using ResidueDisorder

protein	Lindorff-Larsen et al. (Å)	Rosetta ResidueDisorder (Å)
1fme	1.6	2.8
1lmb	1.8	1.6
1mi0	1.2	1.6
1prb	3.3	2.9
2a3d	3.1	2.9
2f21	1.2	1.4
2f4k	1.3	0.8
2hba	0.5	0.6
2jof	1.4	1.2
2p6j	3.6	3.0
2rvd	1.0	1.2
2wxc	4.8	3.4

We also explored whether we could select better (more native-like) structures using the Rosetta score to eliminate structures prior to clustering (rather than the percentage of denatured residues). Similar to the analysis predicting the unfolding events, using the score instead of percent denatured produced results with a comparable accuracy (both identified 7/12 proteins with lower RMSD than the structures selected by Lindorff-Larsen et al.). However, the average RMSD over the 12 proteins was slightly lower when using ResidueDisorder (1.9 Å) than when using the Rosetta score directly (2.0 Å). Table S2 shows the predicted RMSD for each protein.

CONCLUSIONS

Here we present alternative applications for Rosetta ResidueDisorder, expanding on its capability to predict intrinsic disorder from sequence to measure intrinsic disorder directly from structure and also to track changes in conformation for dynamic systems (even for systems that are not intrinsically disordered) by measuring changes in the fraction of denatured residues. Using 229 protein structures, determined by NMR, as a benchmark, we show that ResidueDisorder measured each residue as intrinsically ordered or disordered with an accuracy of 69.2%, 4 percentage points higher than when ResidueDisorder was used to predict intrinsic disorder from sequence (which already outperformed six other prediction methods in our previous study).[14] To our knowledge, Rosetta ResidueDisorder is the first computational tool that can measure intrinsic disorder directly from protein structures. This analysis served as a proof of principle for our next hypothesis, that ResidueDisorder could also be used to track changes in conformation of a protein by measuring the amount of denatured residues. The notion that the method could be used to identify regions of a protein that are intrinsically more conformationally labile from a single static snapshot suggests that the method could be used to infer which regions of a

DOI: 10.1021/acs.jpcb.9b04333
J. Phys. Chem. B 2019, 123, 7103−7112

protein are dynamic and could potentially be involved in rearrangements or serve as regions which conformationally readjust under a biological stimulus.

We also expanded on this ability to determine the percentage of denatured residues by analyzing molecular dynamics trajectories of systems that were not intrinsically disordered. We show that percent of denatured residues in a protein (as calculated using ResidueDisorder) correlated with the RMSD to the native (highly denatured frames also had high RMSD and vice versa) for steered MD, high-temperature, and accelerated MD unfolding trajectories. We also saw the same correlation for long MD trajectories performed near melting temperatures to observe multiple folding/unfolding events. Additionally, we developed methods to identify folding and unfolding events during a trajectory and also predict a native-like structure, which improved the accuracy of the identified native structure compared to when clustering alone was performed. The ability to infer folding/unfolding events from a trajectory may help to determine which regions of proteins are essential or play major roles in defining a protein's fold. Rosetta ResidueDisorder is freely available in the Rosetta software suite as an application. This application was updated to be able to calculate intrinsic disorder directly from structure and also measure percentage of denatured residues from a trajectory of structures as well as to predict folding/unfolding events. In conclusion, we show that Rosetta ResidueDisorder can be used to accurately measure intrinsic disorder of a protein from a static structure (or ensemble of structures). ResidueDisorder can also be applied to analyze molecular dynamics trajectories of non-IDPs to find regions of low RMSD, folding/unfolding events, and a native-like structure throughout conformational changes.

While the current version of ResidueDisorder is limited to studying the behavior of monomers, future work will aim to expand the method to monitor protein−protein interactions as well. Some potential applications could be to examine fuzziness, short linear motifs (SLiMs), and fibril formation. Identification of fuzziness[42,43] for IDPs upon binding to a partner could be examined by identifying regions of IDPs that remain disordered upon binding and encode biological function. ResidueDisorder could potentially be used to examine SLiMs,[44,45] where a short, evolutionarily specific disordered segment of a protein becomes ordered upon binding. Finally, this could be extended to examining changes in disorder of IDPs as they form fibrils (disorder to order transition), as has been done experimentally for alpha synuclein.[19] We believe that this method has the potential to examine any event that can be observed in a molecular dynamics simulation.

■ ASSOCIATED CONTENT

Supporting Information

The Supporting Information is available free of charge on the ACS Publications website at DOI: 10.1021/acs.jpcb.9b04333.

Tables, figures, and a tutorial (PDF)

■ AUTHOR INFORMATION

Corresponding Author

*Phone: 614-292-8284. Fax: 614-292-1685. E-mail: lindert.1@osu.edu.

ORCID

Steffen Lindert: 0000-0002-3976-3473

Notes

The authors declare no competing financial interest.

■ ACKNOWLEDGMENTS

The authors thank D. E. Shaw Research for kindly sharing the long MD trajectories for analysis. We thank members of the Lindert lab for discussions. We also thank the Ohio Five OSU Summer Undergraduate Research Experience (SURE) for giving H.R. the opportunity to work in the Lindert laboratory. We also thank the Ohio Supercomputer Center[46] for valuable computational resources. Work in the Lindert laboratory is supported through the NIH (R03 AG054904, R01 HL137015), the NSF (CHE 1750666), and a Falk Medical Research Trust Catalyst Award.

■ REFERENCES

(1) Oldfield, C. J.; Dunker, A. K. Intrinsically Disordered Proteins and Intrinsically Disordered Protein Regions. *Annu. Rev. Biochem.* **2014**, *83*, 553−584.

(2) Uversky, V. N.; Oldfield, C. J.; Dunker, A. K. Intrinsically Disordered Proteins in Human Diseases: Introducing the D2 Concept. *Annu. Rev. Biophys.* **2008**, *37*, 215−246.

(3) Wright, P. E.; Dyson, H. J. Intrinsically Disordered Proteins in Cellular Signalling and Regulation. Nature Rev. *Nat. Rev. Mol. Cell Biol.* **2015**, *16*, 18−29.

(4) Tompa, P. Intrinsically Disordered Proteins: a 10-year Recap. *Trends Biochem. Sci.* **2012**, *37*, 509−516.

(5) Ferrie, J. J.; Haney, C. M.; Yoon, J.; Pan, B.; Lin, Y.-C.; Fakhraai, Z.; Rhoades, E.; Nath, A.; Petersson, E. J. Using a FRET Library with Multiple Probe Pairs To Drive Monte Carlo Simulations of α Synuclein. *Biophys. J.* **2018**, *114*, 53−64.

(6) Babu, M M.; van der Lee, R.; de Groot, N. S.; Gsponer, J. Intrinsically Disordered Proteins: Regulation and Disease. *Curr. Opin. Struct. Biol.* **2011**, *21*, 432−440.

(7) Uversky, V. N. Introduction to Intrinsically Disordered Proteins (IDPs). *Chem. Rev.* **2014**, *114*, 6557−6560.

(8) Dosztányi, Z.; Csizmok, V.; Tompa, P.; Simon, I. IUPred:web Server for the Prediction of Intrinsically Unstructured Regions of Proteins Based on Estimated Energy Content. *Bioinformatics* **2005**, *21*, 3433−3434.

(9) Ishida, T.; Kinoshita, K. Prediction of Disordered Protein Regions from Amino Acid Sequence. *Nucleic Acids Res.* **2007**, *35*, W460−W464.

(10) Ward, J. J.; McGuffin, L. J.; Bryson, K.; Buxton, B. F.; Jones, D. T. The DISOPRED Server for the Prediction of Protein Disorder. *Bioinformatics* **2004**, *20*, 2138−2139.

(11) Huang, F.; Oldfield, C. J; Xue, B.; Hsu, W.-L.; Meng, J.; Liu, X.; Shen, L.; Romero, P.; Uversky, V. N; Dunker, A; et al. Improving Protein Order-disorder Classification using Charge-hydropathy Plots. *BMC Bioinf.* **2014**, *15*, S4.

(12) Kozlowski, L. P.; Bujnicki, J. M. A Meta-server for the Prediction of Intrinsic Disorder in Proteins. *BMC Bioinf.* **2012**, *13*, 111.

(13) Mizianty, M. J.; Uversky, V.; Kurgan, L. Prediction of Intrinsic Disorder in Proteins using MFDp2. *Methods Mol. Biol.* **2014**, *1137*, 147−162.

(14) Kim, S. S.; Seffernick, J. T.; Lindert, S. Accurately Predicting Disordered Regions of Proteins Using Rosetta ResidueDisorder Application. *J. Phys. Chem. B* **2018**, *122*, 3920−3930.

(15) Fontana, A.; Zambonin, M.; Polverino de Laureto, P.; De Filippis, V.; Clementi, A.; Scaramella, E. Probing The Conformational State of Apomyoglobin by Limited Proteolysis. *J. Mol. Biol.* **1997**, *266*, 223−230.

(16) Wang, R. Y.-R.; Han, Y.; Krassovsky, K.; Sheffler, W.; Tyka, M.; Baker, D. Modeling Disordered Regions in Proteins using Rosetta. *PLoS One* **2011**, *6*, e22060.

(17) Hubbell, W. L.; Gross, A.; Langen, R.; Lietzow, M. A. Recent Advances in Site-directed Spin Labeling of Proteins. *Curr. Opin. Struct. Biol.* **1998**, *8*, 649−656.
(18) Belle, V.; Rouger, S.; Costanzo, S.; Liquière, E.; Strancar, J.; Guigliarelli, B.; Fournel, A.; Longhi, S. Mapping Aalpha-helical Induced Folding within the Intrinsically Disordered C-terminal Domain of the Measles Virus Nucleoprotein by Site-directed Spin-labeling EPR Spectroscopy. *Proteins: Struct., Funct., Genet.* **2008**, *73*, 973−988.
(19) Flynn, J. D.; McGlinchey, R. P.; Walker, R. L., III; Lee, J. C. Structural Features of Alpha-synuclein Fibrils Revealed by Raman Spectroscopy. *J. Biol. Chem.* **2018**, *293*, 767−776.
(20) Simons, K. T.; Bonneau, R.; Ruczinski, I.; Baker, D. Ab Initio Protein Structure Prediction of CASP III Targets using ROSETTA. Ab Initio Protein Structure Prediction of CASP III. *Proteins: Struct., Funct., Genet.* **1999**, *37*, 171−176.
(21) DiMaio, F.; Leaver-Fay, A.; Bradley, P.; Baker, D.; André, I. Modeling Symmetric Macromolecular Structures in Rosetta3. *PLoS One* **2011**, *6*, e20450.
(22) Alford, R. F.; Leaver-Fay, A.; Jeliazkov, J. R.; O'Meara, M. J.; DiMaio, F. P.; Park, H.; Shapovalov, M. V.; Renfrew, P. D.; Mulligan, V. K.; Kappel, K.; et al. The Rosetta All-Atom Energy Function for Macromolecular Modeling and Design. *J. Chem. Theory Comput.* **2017**, *13*, 3031−3048.
(23) Sircar, A.; Chaudhury, S.; Kilambi, K. P.; Berrondo, M.; Gray, J. J. A Generalized Approach to Sampling Backbone Conformations with RosettaDock for CAPRI Rounds 13−19. *Proteins: Struct., Funct., Genet.* **2010**, *78*, 3115−3125.
(24) Guntas, G.; Purbeck, C.; Kuhlman, B. Engineering a Protein-protein Interface using a Computationally Designed Library. *Proc. Natl. Acad. Sci. U. S. A.* **2010**, *107*, 19296−19301.
(25) Meiler, J.; Baker, D. ROSETTALIGAND: Protein−small Molecule Docking with Full Side-chain Flexibility. *Proteins: Struct., Funct., Genet.* **2006**, *65*, 538−548.
(26) Mandell, D. J; Coutsias, E. A; Kortemme, T. Sub-angstrom Accuracy in Protein Loop Reconstruction by Robotics-inspired Conformational Sampling. *Nat. Methods* **2009**, *6*, 551−552.
(27) Siegel, J. B.; Zanghellini, A.; Lovick, H. M.; Kiss, G.; Lambert, A. R.; St. Clair, J. L.; Gallaher, J. L.; Hilvert, D.; Gelb, M. H.; Stoddard, B. L.; et al. Computational Design of an Enzyme Catalyst for a Stereoselective Bimolecular Diels-Alder Reaction. *Science* **2010**, *329*, 309−313.
(28) Aprahamian, M. H.; Chea, E. E.; Jones, L. M.; Lindert, S. Rosetta Protein Structure Prediction from Hydroxyl Radical Protein Footprinting Mass Spectrometry Data. *Anal. Chem.* **2018**, *90*, 7721−7729.
(29) Leelananda, S. P.; Lindert, S. Iterative Molecular Dynamics − Rosetta Membrane Protein Structure Refinement Guided by Cryo-EM Densities. *J. Chem. Theory Comput.* **2017**, *13*, 5131−5145.
(30) Lindert, S.; McCammon, J. A. Improved cryoEM-Guided Iterative Molecular Dynamics − Rosetta Protein Structure Refinement Protocol for High Precision Protein Structure Prediction. *J. Chem. Theory Comput.* **2015**, *11*, 1337−1346.
(31) Lindert, S.; Meiler, J.; McCammon, J. A. Iterative Molecular Dynamics – Rosetta Protein Structure Refinement Protocol to Improve Model Quality. *J. Chem. Theory Comput.* **2013**, *9*, 3843−3847.
(32) Lindorff-Larsen, K.; Piana, S.; Dror, R. O.; Shaw, D. E. How fast folding proteins fold. *Science* **2011**, *334*, 517−520.
(33) Isralewitz, B.; Baudry, J.; Gullingsrud, J.; Kosztin, D.; Schulten, K. Steered Molecular Dynamics Investigations of Protein Function. *J. Mol. Graphics Modell.* **2001**, *19*, 13−25.
(34) Humphrey, W.; Dalke, A.; Schulten, K. VMD - Visual Molecular Dynamics. *J. Mol. Graphics* **1996**, *14*, 33−38.
(35) MacKerell, A. D., Jr.; Banavali, N.; Foloppe, N. Development and Current Status of the CHARMM Force Field for Nucleic Acids. *Biopolymers* **2000**, *56*, 257−265.
(36) Phillips, J. C.; Braun, R.; Wang, W.; Gumbart, J.; Tajkhorshid, E.; Villa, E.; Chipot, C.; Skeel, R. D.; Kale, L.; Schulten, K. Scalable Molecular Dynamics with NAMD. *J. Comput. Chem.* **2005**, *26*, 1781−1802.
(37) Hamelberg, D.; Mongan, J.; McCammon, J. A. Accelerated Molecular Dynamics: A Promising and Efficient Simulation Method for Biomolecules. *J. Chem. Phys.* **2004**, *120*, 11919−11929.
(38) Hamelberg, D.; de Oliveira, C. A. F.; McCammon, J. A. Sampling of Slow Diffusive Conformational Transitions with Accelerated Molecular Dynamics. *J. Chem. Phys.* **2007**, *127*, 155102.
(39) Lindert, S.; Kekenes-Huskey, P. M.; Huber, G.; Pierce, L.; McCammon, J. A. Dynamics and calcium association to the N-terminal regulatory domain of human cardiac troponin C: a multiscale computational study. *J. Phys. Chem. B* **2012**, *116*, 8449−8459.
(40) Wriggers, W.; Stafford, K. A.; Shan, Y.; Piana, S.; Maragakis, P.; Lindorff-Larsen, K.; Miller, P. J.; Gullingsrud, J.; Rendleman, C. A.; Eastwood, M. P.; Dror, R. O.; Shaw, D. E.; et al. Automated Event Detection and Activity Monitoring in Long Molecular Dynamics Simulations. *J. Chem. Theory Comput.* **2009**, *5*, 2595−2605.
(41) Siew, N.; Elofsson, A.; Rychlewski, L.; Fischer, D. MaxSub: an Automated Measure for the Assessment of Protein Structure Prediction Quality. *Bioinformatics* **2000**, *16*, 776−785.
(42) Fuxreiter, M. Fuzziness in Protein Interactions—A Historical Perspective. *J. Mol. Biol.* **2018**, *430*, 2278−2287.
(43) Miskei, M.; Antal, C.; Fuxreiter, M. FuzDB: Database of Fuzzy Complexes, a Tool to Develop Stochastic Structure-function Relationships for Protein Complexes and Higher-order Assemblies. *Nucleic Acids Res.* **2017**, *45*, D228−D235.
(44) Davey, N. E.; Van Roey, K.; Weatheritt, R. J.; Toedt, G.; Uyar, B.; Altenberg, B.; Budd, A.; Diella, F.; Dinkel, H.; Gibson, T. J. Attributes of Short Linear Motifs. Mol. *Mol. BioSyst.* **2012**, *8*, 268−281.
(45) Van Roey, K.; Uyar, B.; Weatheritt, R. J.; Dinkel, H.; Seiler, M.; Budd, A.; Gibson, T. J.; Davey, N. E. Short Linear Motifs: Ubiquitous and Functionally Diverse Protein Interaction Modules Directing Cell Regulation. *Chem. Rev.* **2014**, *114*, 6733−6778.
(46) Ohio Supercomputer Center: Columbus, OH, 1987.

DOI: 10.1021/acs.jpcb.9b04333
J. Phys. Chem. B 2019, 123, 7103−7112